INTERNATIONAL JOURNAL OF GEOMAGNETISM AND AERONOMY
VOL. 3, NO. 2, PAGES 131–139, DECEMBER 2002

MHD model of plasma sheet evolution in an external electric field: Plasma sheet–fast magnetosonic wave interaction

A. V. Runov and M. I. Pudovkin

St. Petersburg State University, St. Petersburg, Russia

Bruno P. Besser

Space Research Institute, Austrian Academy of Sciences, Graz, Austria

Abstract. Results of numerical modelling of plasma sheet dynamics in the presence of an external electric field are discussed. It is shown that the external electric field, fixed on the inflow boundary, expands through the plasma sheet as the fast magnetosonic wave, the front of which switches on plasma convection. This wave carries out the magnetic and total energy fluxes from the inflow boundary to the current sheet, which follows by energy accumulation, current density, and plasma pressure increase in the current sheet. This phase of the process may be associated with the preliminary or growth phase of the magnetospheric substorm. The calculations show that the fast wave front is repeatedly reflected from the neutral line of the sheet as well as from the inflow boundary. As a result, the current density and pressure increases have a jump-like character. As the plasma resistivity dependence on the current density is supposed to have a threshold character, diffusion-type magnetic field reconnection develops when the current density in the sheet exceeds the critical value.

1. Introduction

As is now known, the most powerful space plasma processes occur in the vicinity of relatively small-scale regions, which, following Alfvén, may be called "active regions" [*Alfvén*, 1981]. They may be force-free structures in the solar atmosphere, pinch configurations, or plasma sheets. In any case, the active region is a conditionally stable plasma-magnetic field configuration. The main characteristic feature of objects of such kind is the ability to accumulate magnetic energy as long as the stability conditions are valid. As soon as the stability conditions are violated, the plasma-magnetic field configuration system loses its stability, and the accumulated energy may be released.

This scenario seems to be realized during solar flares and magnetospheric substorms. In the latter case, the magnetotail plasma sheet plays the role of the active region, which is able to accumulate magnetic field energy. The source of the energy may be the solar wind–magnetospheric interaction. This interaction has a complex character and may include the day-side reconnection process as well as quasi-viscous interaction at the magnetopause, and hydrodynamic instabilities that may develop in the solar wind plasma passing by the magnetosphere. All of the processes included produce an electric field in the vicinity of and at the magnetopause. This electric field may locally constrict the plasma sheet of the magnetotail, which is followed by current density enhancement in the sheet, or, similarly, by magnetic energy accumulation. But the increase of the current density or the total pressure gradient may lead to the development of current- or gradient-driven plasma instabilities in the compressed plasma sheet, and to its destruction and subsequent

Paper number GAI01370.
CCC: 1524–4423/2002/0302–0370$18.00

The online version of this paper was published 9 December 2002.
URL: http://ijga.agu.org/v03/gai01370/gai01370.htm
Print companion issued December 2002.

release of the accumulated energy. The first phase of this draft sketch — the phase of energy storage — may be associated with the preliminary or growth phase of the magnetospheric substorm, and the second phase with the substorms' onset.

The scenario roughly prescribed below may correspond to a driven-in or forced magnetic field reconnection process. Driven magnetic reconnection was a subject of many studies. This process was investigated in detail in a set of papers by T. Hayashi and T. Sato [*Hayashi and Sato*, 1978; *Sato*, 1979; *Sato and Hayashi*, 1979] and M. Hoshino [*Hoshino*, 1991]. In all of these papers, the results of MHD numerical simulations are discussed. In the series of T. Hayashi and T. Sato papers, the strong or fast reconnection process model is analyzed. This process is initialized by the plasma and total energy inflow given at the inflow boundary. The initial configuration in this case is not a plasma sheet, but a current sheet with a uniform plasma density distribution. The magnetic field pressure is balanced by a plasma pressure gradient produced by a non-uniform plasma temperature. The density of the inflow plasma is two times the uniform background density. This fast moving flux of dense plasma converges symmetrically to the neutral line and compresses the current sheet. As a result, the temperature (pressure) grows about ten times in the compressed current sheet. The electrical resistivity of the plasma is supposed to be dependent on the current density excess over a given critical value. The intensification of the current sheet followed by resistivity growth results in magnetic field reconnection, high plasma acceleration along the current sheet, and slow-mode shock formation. At a quasi steady-state stage, this process is quite similar to Petschek's model prediction [*Petschek*, 1964].

In contrast, M. Hoshino had considered a slow process. The initial state in his model is the isothermic Harris-type plasma sheet, and the disturbance is given by a small amplitude plasma velocity variation. In this case, there is no dense plasma injection into the plasma sheet, the plasma density increases at the neutral line of the sheet, and it decreases near the inflow boundary — the situation is quite contrary to the Hayashi and Sato model. The electrical resistivity of the plasma is supposed to depend on the magnetic pressure gradient which is a model representation of the low hybrid drift-type (LHD) plasma instability. In the Hoshino model, the resistivity plays a key role. After a long period of plasma sheet compression, the current density at the neutral line of the plasma sheet increases about 10 times. A maximum value of the resistivity normalized to its background value in the vicinity of the neutral line is about 0.0005. So, the inductive electric field in this case is not more than 0.005 normalized units. In Hoshino's model of weak magnetic reconnection, the plasma outflow velocity is about 0.15–0.2 v_a. The resulting magnetic field topology and plasma convection are interpreted as the tearing-mode instability result.

Concerning the plasma sheet in the Earth's magnetotail, Hoshino's model is more preferable. But the substorm onset is a more dynamical process than the process of weak reconnection described by this model.

In both models of strong [*Sato and Hayashi*, 1979] and weak [*Hoshino*, 1991] forced reconnection, only a late stage of the process is studied. In particular, the phase of energy storage in the plasma (current) sheet is not investigated.

As was mentioned in the paper by *Sato and Hayashi* [1979], the process of driven magnetic field reconnection is preceded by a rather long period of magnetic energy accumulation associated with plasma (current) sheet thinning. This process is shown to stop at the moment the current density within the central part of the plasma sheet reaches a critical value corresponding to the development of the hypothetical plasma instability (most probably of LHD or ion-cyclotron type). From the moment of plasma instability development followed by resistivity growth, the reconnection phase of the process is beginning.

In our work, a part of which is presented in this paper, a set of computer experiments was carried out to investigate all phases of the process in detail. At the first part of this set of simulations, the evolution of the simplest plasma sheet configuration, known as the Harris sheet or a flat pinch, used also in the *Hoshino* [1991] model, in the presence of a non-uniform external electric field is modeled. We analyze the fast (strong) regime as well as the slow one. The following question should be answered:

- In what manner does the electric field propagate through the plasma sheet?
- How does the plasma sheet respond to the external non-uniform electric field?
- How does the plasma sheet accumulate the energy?
- How does the accumulated energy get released?

The analysis is based on a numerical solution of the one-fluid nonideal MHD equations. This paper is devoted mainly to the detailed investigation of the first phase of the process: fast wave–plasma sheet interactions.

2. The Model

The simplest current-carrying plasma sheet description known as the "Harris sheet" or "flat pinch" is used as the initial equilibrium state:

$$B_x = B_0 \tanh(z/L)$$
$$j_y = j_0 \mathrm{sech}^2(z/L) \qquad (1)$$
$$p = p_0 \mathrm{sech}^2(z/L)$$

where B_x is the x component of the magnetic field, $B_z = B_y = 0$, j_y is the current density, $j_0 = B_0/\mu_0 L$, p is the plasma pressure, $p_0 = B_0^2/2\mu_0$, L is the characteristic length of the sheet. The x and z coordinates are directed along and across the sheet, correspondingly. It is assumed that there is no dependence of physical values on y, so $\partial/\partial y = 0$. Besides, an unlimited extension of the layer in the x direction is assumed.

The initial steady-state sheet (1) is disturbed by an externally given electric field that has only a y component in the

same direction as the electric current in the plasma sheet. The external electric field is given at the inflow boundary as

$$E_y{}^{in}(x,t)\Big|_{z=\pm 2} = E_0 \mathrm{e}^{(-x/x_l)^2}(1-\mathrm{e}^{-t/t_l}) \tag{2}$$

where E_0 is the given value, which is small compared to the Alfvénic electric field $E_a = v_a B_{x0}$, x_l is the scale of the disturbance in the x direction, and t_l is the disturbance growth time introduced into the model to avoid numerical instabilities. This external electric field gives rise to plasma convection, according to Ohm's law

$$\mathbf{E} + \mathbf{v} \times \mathbf{B} - \eta \mathbf{j} = 0 \tag{3}$$

in dimensionless form, where η is the dimensionless resistivity. It includes the background uniform resistivity, which is supposed to be very small, as well as the current-dependent anomalous resistivity (see details below). The initial state of the plasma sheet and the plasma convection are shown in Figure 1.

It should be noted that this model of the initial disturbance as well as the initial state model essentially differs from the model of the initial state and disturbance used by *Sato and Hayashi* [1979], *Sato* [1979]. The dense plasma inflow is not supposed in our model, in contrast to the *Sato and Hayashi* [1979] model, and we use the isothermal Harris-type plasma sheet, like *Hoshino* [1991], as the initial condition (see Section 1). In our opinion, the model with a plasma sheet and a given external electric field at the boundary as a disturbance is more adequate for the magnetotail situation.

It is presumed that the plasma sheet evolution caused by the disturbance (2) may be described in the MHD approach. The MHD approach is valid if the characteristic scale of the gradients of physical quantities is not less than about 10 Larmor radii. In this case, the plasma sheet evolution is characterized by the following set of equations of one-fluid, nonideal isotropic compressible MHD [*Hayashi and Sato*, 1978; *Scholer et al.*, 1990]:

$$\frac{\partial \rho}{\partial t} = -\nabla \cdot (\rho \mathbf{v}) \tag{4}$$

$$\frac{\partial \rho \mathbf{v}}{\partial t} = -\nabla \cdot (\rho \mathbf{v}\mathbf{v} + (p + \frac{1}{2\mu_0}B^2)\mathbf{I} - \frac{1}{\mu_0}\mathbf{B}\mathbf{B}) \tag{5}$$

$$\frac{\partial \mathbf{B}}{\partial t} = \nabla \times ((\mathbf{v} \times \mathbf{B}) - \eta \mathbf{j}) \tag{6}$$

$$\frac{\partial U}{\partial t} = -\nabla \cdot \mathbf{S} \tag{7}$$

$$\mathbf{j} = \frac{1}{\mu_0}\nabla \times \mathbf{B} \tag{8}$$

$$U = \frac{1}{2}\rho v^2 + \frac{p}{\gamma - 1} + \frac{1}{2}B^2 \tag{9}$$

$$\mathbf{S} = (U + p + \frac{1}{2\mu_0}B^2)\mathbf{v} - \frac{1}{\mu_0}(\mathbf{v} \cdot \mathbf{B})\mathbf{B} + \frac{\eta}{\mu_0}\mathbf{j} \times \mathbf{B} \tag{10}$$

where the magnetic field $\mathbf{B}$ is normalized by the value B_0, ρ is the mass density, $\mathbf{v}$ is the plasma velocity, normalized by $\rho_0 = (\gamma/C_{s\,0}^2)p_0$, where $C_{s0} = (\gamma p_0/\rho_0)^{1/2}$, and $v_a = B_x^0(\mu_0\rho_0)^{-1/2}$; η is the electrical resistivity, normalized by $\eta_0 = \mu_0 L v_a$, and the time is normalized by the Alfvén transport time $t_a = L/v_a$. γ is the polytropic exponent, $\mathbf{I}$ is the unit tensor, and combination **aa** denotes a diad.

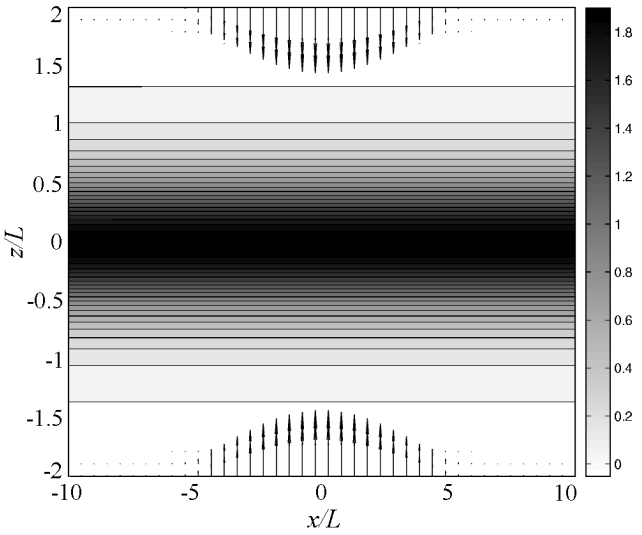

Figure 1. The current density and the plasma flow at $t = 0.025$.

It is assumed, following *Sato and Hayashi* [1979] and *Scholer and Roth* [1987], that plasma electrical resistivity is a threshold-like function of the electric current density:

$$\eta(j) = \begin{cases} \alpha(j - j_c)^2 + \eta_0 & j \geq j_c \\ \eta_0 & j < j_c \end{cases} \tag{11}$$

where α is a coefficient that defines the magnitude of the resistivity, j_c is some critical value of the current density, η_0 is the uniform background resistivity.

As the initial state and the disturbance are symmetric with respect to both the $x = 0$ and $z = 0$ axes, the MHD equation system (3–6) is solved numerically in a rectangular box of 104×104 meshpoints, which corresponds to the upper right quadrant ($x > 0, z > 0$). Besides, the physical computation region $x = [0, 10]$, $z = [0, 2]$ corresponds to a numerical box of 100×100 points, so the mesh size along the x axis equals $\Delta x = 0.1$ and the mesh size along the z axis equals $\Delta z = 0.02$; additional points in both directions are used to construct the boundary conditions. It should be emphasized that the mesh size along the x axis, Δx, is very large, so the numerical resistivity is rather high. However, as we analyze the initial phase of the process (fast wave–plasma sheet interaction), which is not connected to shock-wave generation, the smoothing of plasma parameter gradients associated with the relatively high numerical resistivity is not essential in this case. This value of Δx is used to minimize the run time of the computation. For the analysis of the latest stage of the process connected with magnetic reconnection and slow shock fronts generation, a more dense grid is used.

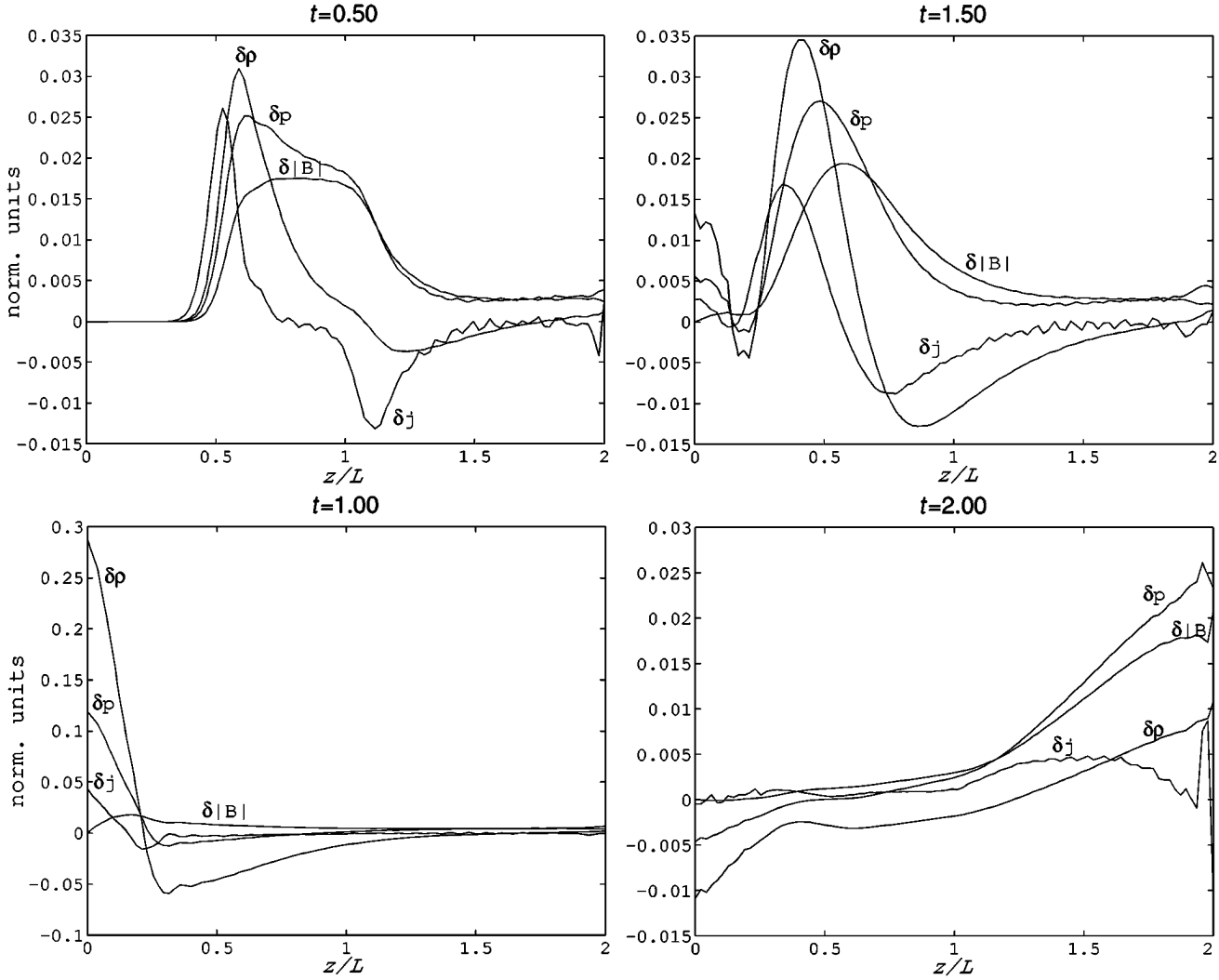

Figure 2. Cross-section profiles of magnetic field intensity ($\delta|B|$), current density (δj), plasma pressure (δp), and density variations ($\delta\rho$) at normalized time units $t = 0.50$, 1.00, 1.50, 2.00.

The boundary conditions are specified for three types of boundaries: the inflow boundary ($z = 2.0$), the free outflow boundary ($x = 10.0$), and two symmetry/antisymmetry boundaries ($x = 0.0$ and $z = 0.0$). The specifications are summarized in Table 1; extrapol. denotes $f_{b+1} = f_b$, where the subscript b denotes the point at the physical boundary, and f corresponds to the value to be computed, and symm./asymm. denote $f_{b+1} = f_{b-1}$ and $f_{b+1} = -f_{b-1}$, correspondingly.

The two-step Lax-Wendroff (LW) numerical scheme is used. A time step of the numerical procedure is determined by the Courant-Friedrichs-Levi stability criterion.

3. Simulation Results

As follows from the previous section, the model has the following set of free parameters: polytropic exponent γ, initial value of the sound velocity C_{s0}, the disturbance magnitude v_0, scale x_l and growth time t_l, the current dependent resistivity coefficient α, and the critical value of the current density j_{cr}. Because a two-dimensional model is considered, the value of γ is taken to be 2 [*Sato and Hayashi*, 1979]. The value of C_{s0} is chosen equal to $(2)^{1/2}$, so the effective temperature $T = p/\rho$ at $t = 0$ equals 1. Other parameters are varied in the set of calculations. The results, discussed below are obtained with $v_0 = 0.05$, $x_l = \alpha = 0.1$, $j_{cr} = 2.50$.

As was mentioned above, the main subject of this study is the early phase of plasma sheet evolution. The first question to be answered is what is the manner in which the electric field, given at the inflow boundary, propagates through the plasma sheet toward the neutral line? In the plots of Figure 2, the cross-section profiles of deviations ($\delta f = f(t + \delta t) - f(t)$, $\delta t = 0.25$, $f = |B|, j_y, \rho, p$) of the absolute value of the magnetic field, current density, plasma density and pressure are shown at normalized time units $t = 0.5, 1.0, 1.5, 2.0$. As can be deduced from Figure 2, the

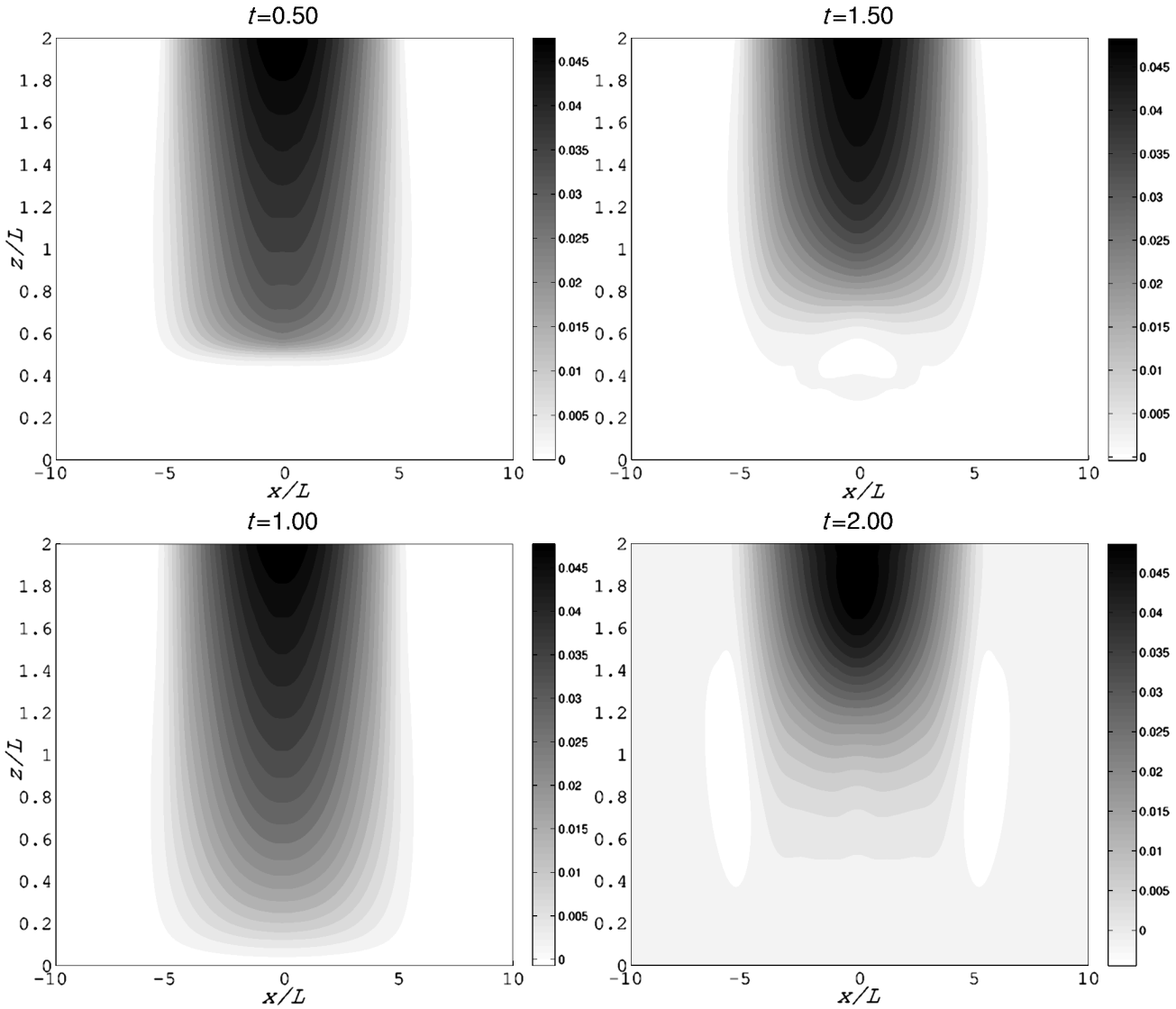

Figure 3. The electric field distribution at normalized time units $t = 0.50, 1.00, 1.50, 2.00$.

disturbance, given at the inflow boundary ($z = 2$), propagates through the plasma sheet toward the neutral line ($z = 0$) as a wave front with cophasal variations of plasma pressure, density, and magnetic field intensity. The velocity of this front motion is approximately equal to the fast magnetosonic wave velocity $v_{fw} = (v_a^2 + c_s^2)^{1/2}$ and equals 3.0 near the inflow boundary and 1.4 in the vicinity of the plasma sheet neutral line (plane).

The positive variation of the current density has its maximum at the front of the wave. Thus, the front of the fast magnetosonic wave is the front of a "switch-on" wave.

It is interesting to note that the configuration of the disturbance profile changes upon moving to the sheet. Indeed, as is seen in the figure, the velocity of the back front of the disturbance is higher than that of the leading front. And as a result, the width of the disturbance along the z axis de-

Table 1. Specifications of the Boundary Conditions

	$z = 0$	$z = 2$	$x = 0$	$x = 10$
v_x	symm.	$\mathbf{v} \times \mathbf{B} = 0$	symm./antisymm.	extrapol.
v_z	symm./antisymm.	inflow (2)	symm.	extrapol.
B_x	symm./antisymm.	extrapol.	symm.	extrapol.
B_z	$\nabla \times \mathbf{B} = 0$	$\nabla \times \mathbf{B} = 0$	$\nabla \times \mathbf{B} = 0$	$\nabla \times \mathbf{B} = 0$

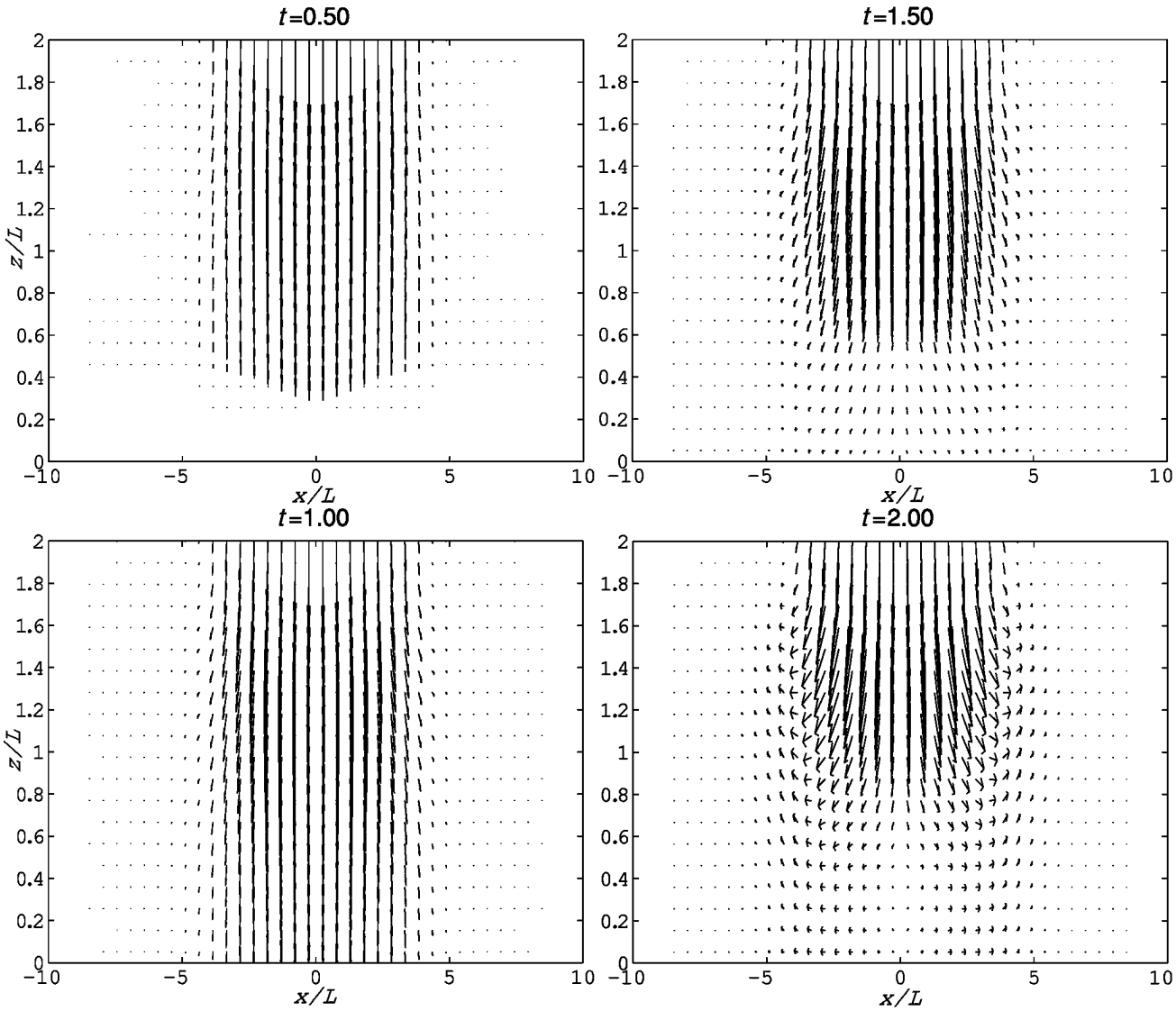

Figure 4. The plasma convection distribution at normalized time units $t = 0.50$, 1.00, 1.50, 2.00.

creases with time, so that in the vicinity of the current sheet, the extension of the disturbance along the z axis proves to be about $\Delta z = (0.3 - 0.4)L$.

The two-dimensional distribution of the electric field in the motionless frame of reference at time instances $t = 0.50$, 1.00, 1.50, and 2.00 of the normalized time is displayed in Figure 3. The electric field, expanding from the inflow boundary inward as the fast-wave front, switches on the plasma convection. The plasma velocity vector distributions at the same moments are shown in Figure 4.

At this point, it must be noted that though the plasma convection front moves at the fast magnetosonic wave speed, the plasma behind it is moving with the electric drift velocity, which is much less than the wave front velocity.

The calculations show that the fast magnetosonic wave is reflected from the plasma sheet neutral plane after the front reaches it and moves backward to the inflow boundary. Then, as the electric field is supposed to be constant in time at the inflow boundary, the wave front is reflected from the boundary and moves toward the neutral line again. This process has a well pronounced quasi-recurrent character. It should be noted that the change of front motion direction, described below, is not followed by the change of electric field and, correspondingly, plasma convection direction. For the entire period under consideration, the plasma generally flows toward the neutral line. However, the reflection of the disturbance from the current sheet is essentially "inelastic," that is, the interaction of the disturbance with the sheet results in a noticeable change of the parameters of the latter. In particular, the current intensity, plasma density and pressure increase by the values of $\Delta j = 0.003$, $\Delta\rho \simeq 0.03$, and $\Delta p = 0.005$, correspondingly. As a result, after a series of wave bounces, the magnetic energy of the system essentially increases. Besides, as may be seen in the

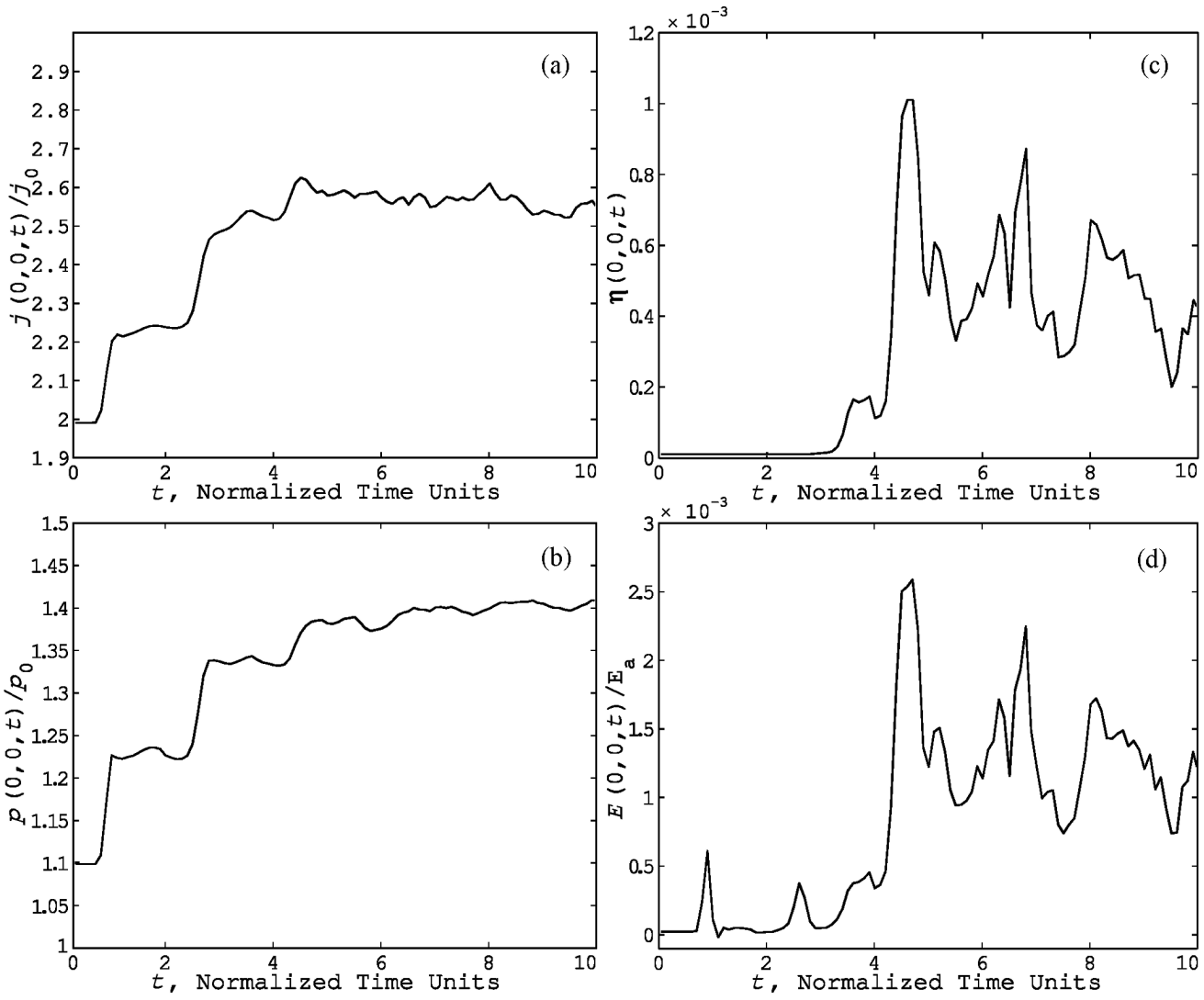

Figure 5. The temporal variation of the current density (a), plasma pressure (b), current-dependent resistivity (c), and electric field (d) at the origin (0,0).

graphics presented in Figure 4, a remarkable x component of the plasma velocity appears. At $t = 2.0$, the plasma flow shows a vortex character. The vortices of plasma convection at $x = \pm 2.5 - \pm 5.0$ are associated with regions of the negative electric field (Figure 3).

As the results of the calculations show, the magnetic energy continuously increases at all points at the cross-sheet profile until $t \simeq 4.0$. After that moment, the magnetic energy increase stops, and the process approaches and proceeds in a steady-state regime (analogy of the stationary convection in the magnetotail plasma sheet), and the plasma convection exhibits a quasi-hyperbolic character. Taking into account that energy continues to enter the system, one may suppose that the energy input is balanced by an increased output rate during this period. The physical mechanism of the increase of the energy output rate may be understood from the data presented in Figure 5, where graphics of time variations of the current density (upper panel), current-dependent resistivity, the electric field, and the plasma pressure at the point $x = 0, z = 0$ are presented. As is seen from the presented data, the current density at the axis of the sheet grows in a step-like manner until $t \simeq 4.5$, and at $t \geq 3$ the current density in the region of maximal compression of the sheet reaches and then exceeds the critical value $j_{cr} = 2.50$. According to the model, this has to result in a burst-like increase of the plasma resistivity and intensification of the magnetic field reconnection process. In accordance with equation (11), the "anomalous" resistivity η develops at $t \simeq 4$, when the current density approaches the threshold value j_{cr}, then the resistivity significantly grows with a peak at $t \simeq 4.5$. It is interesting to note that in spite of a rapid increase of plasma resistivity, the current density also increases at that time, which supposes a corresponding increase of electric field intensity. And indeed, as may be

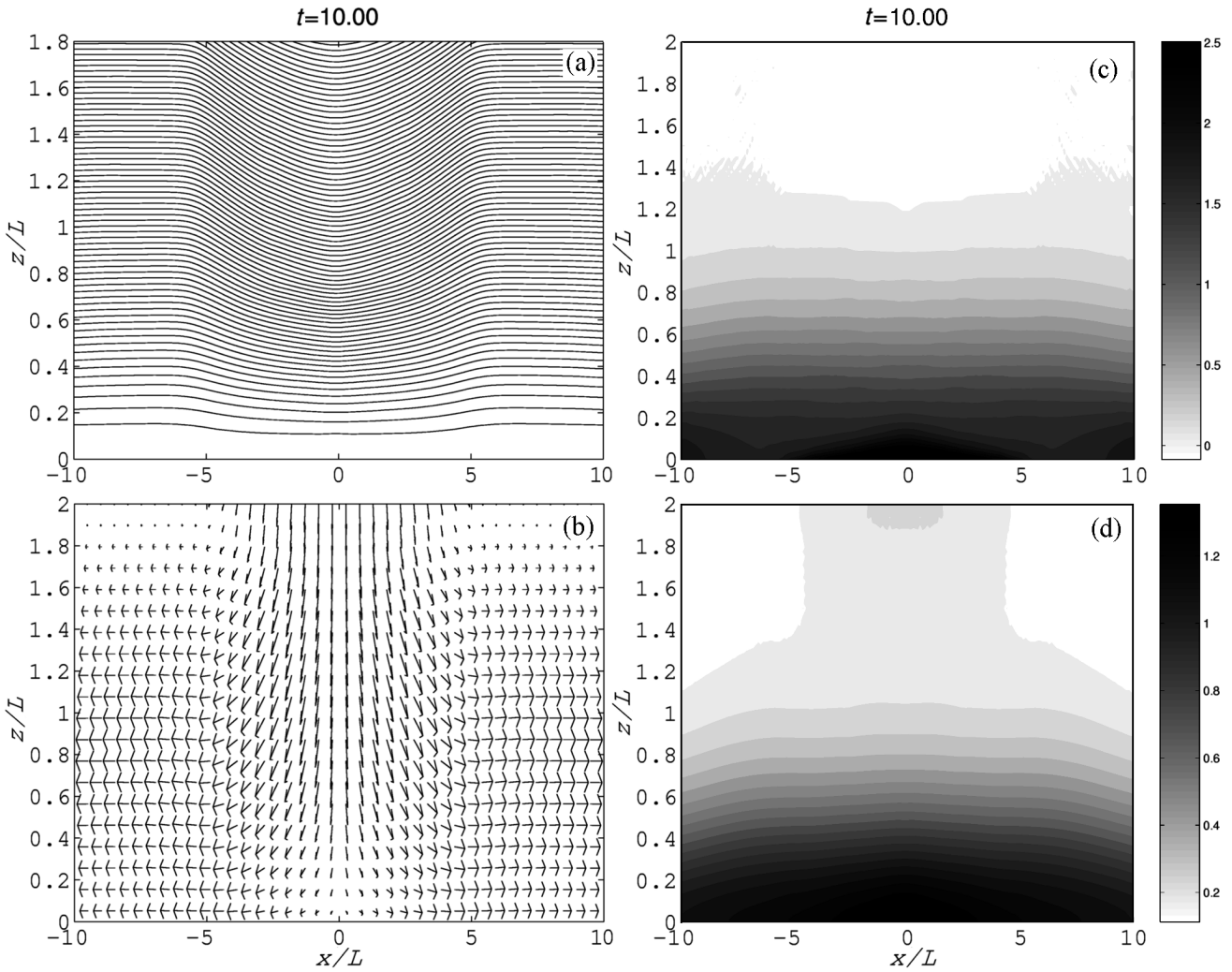

Figure 6. The magnetic field configuration (a), plasma convection (b), current density (c), and plasma pressure (d) distributions at normalized time $t = 10.00$.

seen from the results presented, the time variation of the electric field at the vicinity of the point (0,0) is completely determined by the time behavior of the current-dependent resistivity. In particular, a jump of η at $t = 4$ results in a corresponding jump of the E field. And though the E field intensity at this point is much lower than E_0 at the inflow boundary, it is sufficient to provide the necessary increase of the plasma and energy outflow. Further variations of the resistivity and the electric field in the region of maximal compression of the plasma sheet are characterized by a set of quasi-recurrent activations with decreasing amplitude.

The plasma pressure also grows significantly during the period $0 < t \leq 5$. At $t > 5$, the plasma pressure growth becomes much slower, with a distinct quasi-periodic variation (see Figure 5).

The magnetic field configuration, plasma convection, current density, and plasma pressure at $t = 10.0$ are shown in Figure 6. As is seen in the figure, the reconfiguration of the plasma flow associated with the propagation of the external electric field into the plasma sheet results in the formation of a quasi-hyperbolic plasma flow all over the system under consideration without any shock wave appearance. At the same time, the magnetic field line structure is characterized by the existence of a neutral line of X type, which may be considered as obvious evidence for magnetic field reconnection development. On the whole, the magnetic field–plasma convection system corresponds to that in the Sweet–Parker problem rather than that of the Petschek model. This situation seems to be associated first of all with a rather large numerical viscosity of the calculation scheme that results in a relatively small increase of the current–driven plasma resistivity (by about an order of magnitude).

The other circumstance leading to this situation is a rather small scale of the external electric field in the x direction, which results in a correspondingly extensive stretching of the compressed current layer in the x direction.

4. Discussion and Conclusions

As follows from the results presented above, the external electric field given at the inflow boundary propagates through the plasma sheet as the fast magnetosonic wave. The front of that wave switches on plasma convection and the Pointing vector flux and thereby provides the energy input into the current sheet. A very interesting feature of the electric field penetration into the plasma sheet is repeated reflection of the wave front from the current sheet and the inflow boundary. Every act of the front reflection from the current sheet manifests itself in a pulse of the electric field intensity, current density, and plasma pressure jump at the neutral line of the sheet. It seems tempting to suppose that repeated intensifications of equatorward-moving auroral arcs observed during the preliminary phase of substorms may be associated with an analogous process within the magnetospheric plasma sheet. At the same time, the reflections of the wave front from the current sheet are not associated with the change of the sign of the electric field. Correspondingly, the Pointing vector provides a continuous energy input into the current sheet and the increase of the current intensity up to the values exceeding the plasma stability threshold value. This, in turn, results in the development of the anomalous resistivity, formation of a magnetic X line, and onset of the magnetic reconnection process. All these features of the process developing during the initial phase of the plasma sheet evolution seem to be peculiarly independent of the geometrical characteristics of the current sheet and the electric field intensity E_0.

However, the intensity and properties of the subsequent reconnection process in the case under consideration are rather special: as is seen in Figure 5, the maximum value of the electric field within the current sheet is about $2.5 \times 10^{-3} E_a$. Besides, the reconnection process is not associated with the formation of any shock waves. And, finally, the reconnection process is not followed by any visible decrease of the accumulated magnetic energy.

All these peculiarities of the magnetic reconnection in the model discussed may be explained by two factors.

As was stated above, a relatively high numerical resistivity of the plasma results in a correspondingly low jump of resistivity described by equation (11).

This, in turn, results in a rather small variation of the current density and magnetic field intensity, in particular, in a small z component of the magnetic field in the reconnection region. Then, in the expression for the y component of the electric field within the current sheet $E = \eta j + v_x B_z$, the last term on the right-hand side may be neglected, and the electric field variation is described mainly, in accordance with Figure 5, by the first term: $E = \eta j$. Thus, the magnetic field reconnection in the current sheet with the chosen input parameters corresponds on the whole to the Sweet-Parker model rather than to the Petschek model.

At the same time, the solution obtained allows one to formulate the conditions favorable for a model of fast Petschek-type reconnection. First of all, it is necessary to decrease the numerical resistivity. Besides, it would be necessary to decrease the value of the ratio z_b/L, which will result in a more narrow localization of the region of fast wave interaction with the current sheet, and, correspondingly, in a smaller scale of the diffusion region.

Results of the calculations will be presented in a subsequent paper.

Acknowledgment. This work was supported by the Russian Foundation for Basic Research, grants No. 99-05-04006 and No. 00-05-64894.

References

Alfvén, H., *Cosmic Plasma*, D. Reidel Publishing Company, Dordrecht, Holland, 1981.

Hayashi, T., and T. Sato, Magnetic reconnection: Acceleration, heating and shock formation, *J. Geophys. Res., 83*, 217, 1978.

Hoshino, M., Forced magnetic reconnection in a plasma sheet with localized resistivity profile excited by lower hybrid drift type instability, *J. Geophys. Res., 96*, 11,555, 1991.

Petschek, H. E., Magnetic field annihilation, in *Proceedings of the AAS-NASA Symposium on Physics of Solar Flares, NASA Spec. Publ., 50*, 425, 1964.

Sato, T., Strong plasma acceleration by slow shocks resulting from magnetic reconnection, *J. Geophys. Res., 84*, 7177, 1979.

Sato, T., and T. Hayashi, Externally driven magnetic reconnection and a powerful magnetic energy convertor, *Phys. Fluids, 22*, 1189, 1979.

Scholer, M., and D. Roth, A simulation study on reconnection and small-scale plasmoid formation, *J. Geophys. Res., 92*, 3223, 1987.

Scholer, M., T. Terasawa, and F. Jamitzky, Reconnection and fluctuations in compressible MHD: A comparison of different numerical methods, *Comput. Phys. Commun., 59*, 175, 1990.

A. V. Runov and M. I. Pudovkin, Institute of Physics, St. Petersburg State University, St. Petersburg, Petrodvorets 198904, Ulyanovskaya 1, Russia. (pudovkin@geo.phys.spbu.ru)

Bruno P. Besser, Space Research Institute, Austrian Academy of Sciences, Graz, Austria.

(Received 12 April 2001; accepted 26 September 2002)